

DOI: 10.15825/1995-1191-2025-1-103-113

CHEMICAL DECELLULARIZATION OF PORCINE LIVER BY TWO-STAGE TREATMENT WITH SURFACTANTS AND OSMOREGULATORS ENHANCES PRESERVATION OF LIVER EXTRACELLULAR MATRIX STRUCTURE

A.D. Belova¹, E.A. Nemets¹, D.D. Filin¹, A.S. Ponomareva¹, L.A. Kirsanova¹, Yu.B. Basok¹, V.I. Sevastianov^{1, 2}

¹ Shumakov National Medical Research Center of Transplantology and Artificial Organs, Moscow, Russian Federation

² Institute of Biomedical Research and Technology, Moscow, Russian Federation

Objective: to develop and investigate a tissue-specific matrix obtained using a modified chemical porcine liver decellularization regime in order to effectively increase preservation of extracellular matrix (ECM) structure, reduce decellularization time and improve purification of the ECM from cellular elements. **Materials and methods.** Original porcine liver was minced to obtain tissue fragments. Five decellularization regimes were used, with the concentrations and timing of surfactant treatments varied: 0.1% sodium dodecyl sulfate (SDS) and 0.1% or 1% Triton X-100, without and in combination with phosphate-buffered saline (PBS). The glycosaminoglycan (GAG) content of the resulting fragments was determined by lysing the samples for 12 hours in papain solution at +65 °C and then incubating them in 1,9-dimethylmethylene blue. DNA quantification was carried out using DNeasy Blood&Tissue Kit and Quant-iT PicoGreen dye. The morphology of the samples was studied using histological staining techniques. Cytotoxicity of the samples *in vitro* was evaluated on an NIH/3T3 mouse fibroblast culture by direct contact. **Results.** Treatment with 0.1% SDS for 2.5 hours with additional treatment with 1% Triton X-100 containing PBS for 21.5 hours (regime 4) increased GAG content to $11.66 \pm 0.61 \mu\text{g}/\text{mg}$ compared to $0.68 \pm 0.06 \mu\text{g}/\text{mg}$ (regime 5). The DNA content of samples obtained in regime 4 decreased from $99.75 \pm 3.93 \text{ ng}/\text{mg}$ to $14.93 \pm 4.91 \text{ ng}/\text{mg}$ after additional treatment with type I DNase, indicating that cellular components were effectively removed. This matrix showed no cytotoxicity. **Conclusion.** By optimizing the chemical decellularization regime for porcine liver, we were able to improve preservation of ECM structures, shorten decellularization time and effectively reduce the content of cellular elements. The modified decellularization protocol allowed to obtain a non-cytotoxic tissue-specific matrix with a low potential immunogenicity and a more preserved ECM structure and higher GAG content.

Keywords: porcine liver, decellularization, glycosaminoglycans, tissue engineering.

INTRODUCTION

Over the last decade, tissue engineering has advanced significantly, with cell-free matrices obtained through decellularization becoming a cornerstone among biodegradable materials used as cellular carriers in cell-engineered constructs. Bioequivalents of liver tissue serve as both a promising alternative to liver transplantation – helping address the global donor organ shortage – and as effective *in vitro* models for drug screening and personalized medicine.

The primary advantages of using matrices derived from decellularized organs include: their ability to preserve the native extracellular matrix (ECM) structure and biochemistry, effectively providing a near-native microenvironment for cells to repopulate and function within; low immunogenicity achieved by removing cellular components; high biocompatibility; potential for

xenogeneic organ utilization for decellularization [1, 2]. In this context, matrices derived from decellularized tissues and organs serve not only as physical scaffolds for cells but also actively support their proliferation and function [3, 4]. A key objective in developing decellularization protocols is the preservation of glycosaminoglycans (GAGs), a major ECM component. GAGs are essential for cell adhesion, proliferation, and differentiation [5], largely due to their ability to interact with cytokines, growth factors, enzymes, and proteins [6].

The choice of a decellularization method depends on several factors, including the specific organ type, species origin, tissue structure, and density. Decellularization techniques are generally classified into physical, chemical, and enzymatic methods [7, 8].

Among chemical approaches, Triton X-100 and sodium dodecyl sulfate (SDS) are commonly used to dis-

Corresponding author: Aleksandra Belova. Address: 1, Shchukinskaya str., Moscow, 123182, Russian Federation. Phone: (963) 633-94-34. E-mail: sashak1994@mail.ru

rupt cell membranes and denature proteins effectively. Triton X-100, a non-ionic detergent, is considered less aggressive toward collagen, elastin, and GAGs in ECM compared to SDS [9, 10]. Due to its ionic nature, SDS requires extensive washing to prevent cytotoxic residues from remaining deep within the tissue, as their removal can be challenging [11–13].

To enhance cell membrane permeability and improve surfactant penetration deep into the tissue, decellularization protocols often leverage a synergistic approach by combining multiple methods [14, 15].

For instance, to enhance the efficiency of the decellularization process in mouse liver tissue, Kobes et al. combined surfactants with osmotic shock-inducing substances [16]. Osmotic shock, achieved through alternating hypertonic and hypotonic solutions, promotes cell lysis while minimally affecting the ECM and facilitates the removal of cell debris post-lysis [17, 18]. Similarly, Suss et al. employed an SDS solution supplemented with EDTA and ultrasound to decellularize nervous tissue [19].

Previously, we proposed a protocol for generating a tissue-specific microdispersed matrix from decellularized liver using a prolonged (72-hour) treatment with three surfactant solutions containing SDS and increasing Triton X-100 concentrations, followed by DNase treatment [20, 21]. This approach effectively removes cellular components while leveraging Triton X-100 to aid in the removal of SDS residues [12]. However, drawbacks include the extended duration of the decellularization process and the use of a magnetic stirrer, which may negatively impact the ECM's composition and structural integrity.

This study aimed to develop and evaluate a tissue-specific matrix derived from porcine liver using a modified chemical decellularization protocol. The proposed approach focuses on enhancing ECM preservation, shortening decellularization time, and improving the removal of cellular components from ECM.

MATERIALS AND METHODS

Object of study

For decellularization we used porcine liver obtained at a slaughterhouse (PROMAGRO, Stary Oskol) after slaughtering the healthy animals. The original tissue was frozen at $-20\text{ }^{\circ}\text{C}$. Before the experiments, the liver was

defrosted and mechanically minced using a scalpel and scissors to obtain porcine liver fragments (PLF) no larger than $1.5\times 1.5\text{ mm}$.

PLF decellularization regimes

PLF were processed using 5 decellularization regimes at $+25\text{ }^{\circ}\text{C}$ and constant stirring at 90 rpm using an ES-20/60 incubator shaker (Biosan, Latvia). The decellularization regimes are presented in Table.

In all protocols, the PLF underwent sequential treatment with a surfactant-containing solution in distilled water, followed by phosphate-buffered saline (PBS; 137 mM NaCl, 2.67 mM KCl, 1.47 mM KH_2PO_4 , 8.1 mM Na_2HPO_4 , pH 7.4) containing surfactant (low ionic strength solution) for a specified duration.

PLF treatment with DNase

To achieve complete removal of cellular components, as assessed by the residual DNA, after decellularization of samples in regime 4, we included an additional PLF treatment with a type I DNAase solution (SayStorLab, Russia). Samples (0.5 ml) were placed in 1.0 mL of 10 mM Tris-HCl pH 7.6 solution containing 2.5 mM MgCl_2 , 0.5 mMol CaCl_2 , and 50 U/mL DNAase I and incubated for 48 hours at $+37\text{ }^{\circ}\text{C}$.

Determination of glycosaminoglycan content in native liver and decellularized PLF

For quantification of GAG content in native and decellularized PLF (DPLF), samples were lyophilized at $-80\text{ }^{\circ}\text{C}$ (FreeZone, Labconco, USA). After lyophilization, 30 mg samples each ($n = 3$) were lysed in papain solution (Sigma-Aldrich, USA) at $+65\text{ }^{\circ}\text{C}$ for 12 hours. GAG concentration was measured using 1,9-dimethylmethylene blue (DMMB) dye (Sigma-Aldrich, USA) and a Tecan Spark 10M tablet reader (Tecan Trading, Switzerland), measuring absorbance at 525 nm wavelength.

Double-stranded DNA staining with DAPI dye in native liver and DPLF

For preliminary assessment of DNA content in native porcine liver ($n = 3$) and DPLF ($n = 3$), samples were pre-frozen at $-20\text{ }^{\circ}\text{C}$, embedded in freezing medium (Leica, Germany), and sectioned into 10- μm -thick slices using a Leica CM1900 UV cryostat microtome (Leica,

Table

Porcine liver decellularization regimes

Regime	Stage I	Stage II
1	$\text{H}_2\text{O} + \text{SDS } 0.1\% - 2.5\text{ hours}$	$\text{PBS} + \text{SDS } 0.1\% - 21.5\text{ hours}$
2	$\text{H}_2\text{O} + \text{Triton X-100 } 0.1\% - 2.5\text{ hours}$	$\text{PBS} + \text{Triton X-100 } 0.1\% - 21.5\text{ hours}$
3	$\text{H}_2\text{O} + \text{Triton X-100 } 1\% - 2.5\text{ hours}$	$\text{PBS} + \text{Triton X-100 } 1\% - 21.5\text{ hours}$
4	$\text{H}_2\text{O} + \text{SDS } 0.1\% - 2.5\text{ hours}$	$\text{PBS} + \text{Triton X-100 } 1\% - 21.5\text{ hours}$
5	$\text{H}_2\text{O} + \text{Triton X-100 } 1\% - 18\text{ hours}$	$\text{PBS} + \text{SDS } 0.1\% - 6\text{ hours}$

Note: SDS, sodium dodecyl sulfate; PBS, phosphate-buffered saline.

Germany). The sections were then stained with the blue-fluorescent DNA stain 4',6-diamidino-2-phenylindole (DAPI) (Sigma-Aldrich, USA) at a concentration of 1 µg/mL. Each sample was visually examined for DNA preservation using a Leica THUNDER Imager fluorescence microscope (Leica, Germany).

Quantification of DNA in native liver and DPLF

To quantify DNA content in native liver and DPLF samples, the DNeasy Blood & Tissue Kit (QIAGEN, Germany) was used following the manufacturer's instructions. A 10 mg sample of native liver (n = 3) or DPLF (n = 3) was processed for analysis. Double-stranded DNA quantification was performed using the QuantiT PicoGreen dsDNA Assay Kit and dsDNA Reagents (Invitrogen, USA) according to the manufacturer's protocol. DNA content in the samples was measured using a Tecan Spark 10M microplate reader (Tecan Trading AG, Switzerland) at a wavelength of 520 nm.

Determination of *in vitro* cytotoxicity of DPLF

In vitro cytotoxicity of DPLF samples was assessed following the interstate standard GOST ISO 10993-5-2011 [22] using NIH/3T3 mouse fibroblasts (ATCC® CRL-1658™, American Type Culture Collection) and the direct contact method. Fibroblasts were cultured in standard 25 cm² culture flasks (CELLSTAR Greiner Bio-One, Germany) with complete growth medium (CGM) containing DMEM (Dulbecco's Modified Eagle's Medium) with high glucose (4.5 g/L, DMEM high glucose c HEPES, PanEco, Russia), 10% calf serum (Biosera, Germany), Anti-Anti antibiotic-antimycotic (Gibco, Thermo Fisher Scientific, USA), and 2 mM glutamine (PanEco, Russia). Cultures were maintained in a CO₂ incubator at 37 °C under a humidified atmosphere with (5 ± 1)% CO₂. Cells were detached using TrypLE Express Enzyme dissociation reagent (Gibco, Thermo Fisher Scientific, USA), and the initial cell count was determined using a TC 20™ Automated Cell Counter (Bio-Rad Laboratories Inc., USA). The initial cell count in the suspension was determined using a TC 20™ Automated Cell Counter (Bio-Rad Laboratories Inc., USA). To assess cytotoxic effects, fibroblasts were seeded into 96-well flat-bottomed culture plates (CELLSTAR Greiner Bio-One, Germany) at a concentration of 1–2 × 10⁶ cells per well and incubated in CGM under standard conditions until an (80 ± 10)% monolayer was established. Test samples (n = 8) were then introduced into wells containing the fibroblast monolayer and incubated for 24 hours. Morphological changes in fibroblasts were assessed using a Nikon Eclipse TS100 microscope (Nikon, Japan).

To evaluate the effect of DPLF samples on NIH/3T3 cell viability, cells were stained using the LIVE/DEAD Cell Viability/Cytotoxicity Kit (Molecular Probes by Life Technologies, USA) following the manufacturer's

protocol. Fluorescence analysis was conducted using a Nikon Eclipse Ti fluorescence microscope (Nikon, Japan).

As controls, nutrient medium DMEM with a high glucose content of 4.5 g/L (PanEco, Russia) served as the negative control to establish baseline cellular responses, while a single-element aqueous zinc standard (10,000 µg/mL, Sigma-Aldrich, USA) was used as the positive control.

Histological examination of native liver and DPLF

Samples of native liver tissue and DPLF were fixed in a 10% formalin solution, washed in running water, and dehydrated using a graded ethanol series. They were then treated sequentially with an ethanol-chloroform mixture, pure chloroform, and finally embedded in paraffin.

Histological sections were deparaffinized, rehydrated, and stained using hematoxylin and eosin for general tissue structure, Masson's method for total collagen content, and alcian blue for GAGs. The stained sections were analyzed and photographed using a Nikon Eclipse Ti inverted microscope (Nikon, Japan).

Statistical analysis of obtained results

Data analysis was performed using Microsoft Office Excel (2021). Mean values and standard deviations were calculated, and statistical significance was assessed using Student's t-test. A p-value of <0.05 was considered statistically significant.

RESULTS AND DISCUSSION

Fig. 1 illustrates the impact of different porcine liver decellularization protocols (outlined in Table) on GAG concentration in DPLF samples. For comparison, the figure also includes data from DPLF obtained using a previously developed protocol involving magnetic stirring [20, 21]. It is known that GAG content in native porcine liver tissue is lower (0.59 ± 0.03 µg/mg dry tissue) than in decellularized samples, likely due to the high cellular mass fraction in the liver (comprising up to 80% of the organ's total mass) [23].

When liver fragments were treated with 0.1% SDS for 24 hours (regime 1), only a small amount of GAG was retained (3.42 ± 1.03 µg/mg dry tissue), which was not significantly different from the previously developed protocol (3.03 ± 0.24 µg/mg dry tissue) [20, 21]. Notably, several studies have also reported the detrimental effect of SDS on GAG retention during decellularization of various tissues and organs [24, 25]. An evaluation of the effect of Triton X-100 at 0.1% (regime 2) and 1% (regime 3) concentrations – used to enhance cell membrane permeability and promote cell lysis – revealed no significant difference in GAG retention, with values of 9.38 ± 0.67 µg/mg dry tissue and 10.74 ± 0.95 µg/mg dry tissue, respectively.

After decellularization under regimes 3 and 4, residual GAG content did not differ significantly (10.74 ± 0.95 $\mu\text{g}/\text{mg}$ dry tissue and 11.66 ± 0.61 $\mu\text{g}/\text{mg}$ dry tissue, respectively). However, in regime 5 – where 1% Triton X-100 was used in the first stage (18 hours) followed by 0.1% SDS in the second stage (6 hours) – GAG retention was the lowest, at 0.68 ± 0.06 $\mu\text{g}/\text{mg}$ dry tissue.

Beyond maintaining ECM structure and key components, effective decellularization requires the thorough removal of cells and cellular debris. A key indicator of successful decellularization is the absence of nuclear material, as confirmed by DAPI staining. DAPI selectively binds to double-stranded DNA, producing fluorescence that is twenty times more intense upon binding, making it a reliable marker for residual nuclear content (Fig. 2, a–e) [18].

As shown in Fig. 2, a, the characteristic fluorescence of nuclei was clearly detected in the original porcine liver tissue. In DPLF samples, the intensity of fluorescence varied depending on the decellularization regime and the effectiveness of cellular removal. In regime 1 (Fig. 2, b), a moderate number of visible nuclei remained, indicating partial decellularization. Similarly, regimes 2 and 3 (Fig. 2, c, d), which used only Triton X-100, resulted in multiple observable nuclei, demonstrating that this surfactant alone is insufficient for complete cellular removal. In contrast, regime 4 (Fig. 2, e), which involved sequential treatment with 0.1% SDS followed by 1% Triton X-100, showed a significant reduction in nuclear content. Notably, regime 5, which reversed the order – starting with 1% Triton X-100 followed by 0.1% SDS – resulted in the complete absence of visible nuclei, indicating the most effective decellularization.

Application of all decellularization regimes significantly reduced the DNA content in DPLF compared to the original liver tissue (Fig. 2, g), an essential factor in minimizing the potential immunogenicity of the matrix. According to the criteria proposed by Crapo et al., a decellularized matrix is considered adequately processed if it contains no more than 50 ng of DNA per mg of tissue. Triton X-100 and SDS are known to remove up to 90% of DNA from tissue [18, 26].

In regime 1, where the sample was treated with 0.1% SDS solution, the DNA content was reduced to 34.78 ± 3.82 ng/mg dry tissue – just 2.18% of the DNA present in the original liver tissue (1595.10 ± 96.80 ng/mg dry tissue). The significant reduction in DNA observed with regime 1 likely results from the synergistic effect of SDS-induced changes in osmotic strength, which enhances cell membrane destruction and promotes more efficient cell lysis.

The use of other decellularization regimes did not achieve the minimum DNA removal threshold of 50 ng/mg tissue. This suggests that additional steps are needed to improve the penetration of decellularizing agents deep into the matrix, facilitating cell membrane destruction and cell lysis.

It is worth noting that treating tissue with only 0.1% or 1.0% Triton X-100 solutions is often insufficient for complete cell removal. While these treatments preserve high GAG content (9.38 ± 0.67 $\mu\text{g}/\text{mg}$ dry tissue and 10.74 ± 0.95 $\mu\text{g}/\text{mg}$ dry tissue, respectively), they fail to eliminate sufficient amounts of genetically active material. A similar trend was observed in decellularization regime 4, where sequential exposure to 0.1% SDS and 1% Triton X-100 reduced DNA levels only to

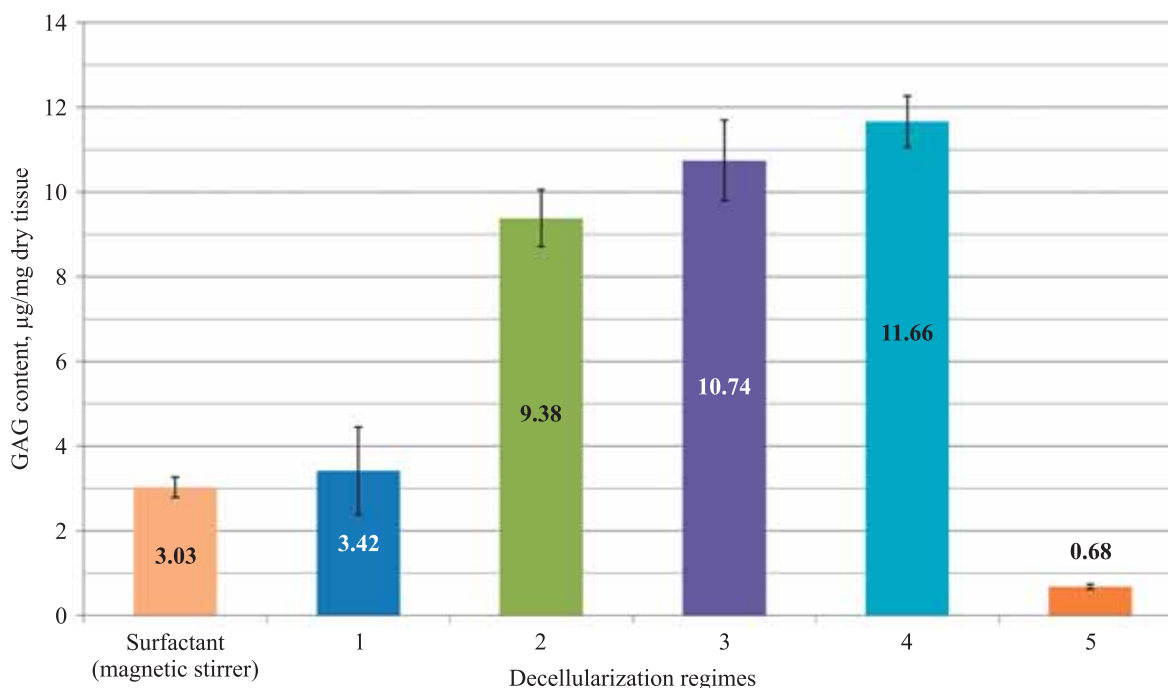


Fig. 1. Effect of porcine liver decellularization regime on GAG content

99.75 ± 3.93 ng/mg dry tissue – well above the required threshold. However, this protocol retained the highest GAG content (11.66 ± 0.61 µg/mg dry tissue).

Histological staining of DPLF samples was performed to validate the results obtained. Two samples were selected for examination based on their distinct characteristics: regime 1, which achieved the lowest residual DNA content, ensuring effective cell removal, and regime 4, which preserved the highest amount of GAG within the DPLF-based matrix (Fig. 3).

When stained with hematoxylin and eosin, as well as using the Masson method, the sample treated under regime 1 exhibited polymorphic fragments of decellularized liver with a well-preserved intra-lobular structure

and pronounced porosity (Fig. 3, a, b). This structural integrity could positively impact DPLF recellularization, as high porosity facilitates nutrient diffusion to cells within the matrix and supports neovascularization.

Additionally, no preserved cell nuclei or cellular debris were observed in the sample, corroborating the quantification of residual DNA, which indicated minimal genetic material remaining post-decellularization. However, GAG staining with alcian blue was very weak (Fig. 3, c), aligning with the low quantified GAG content. This suggests that regime 1 – while effective in DNA removal – led to significant loss of GAG, a crucial ECM component.

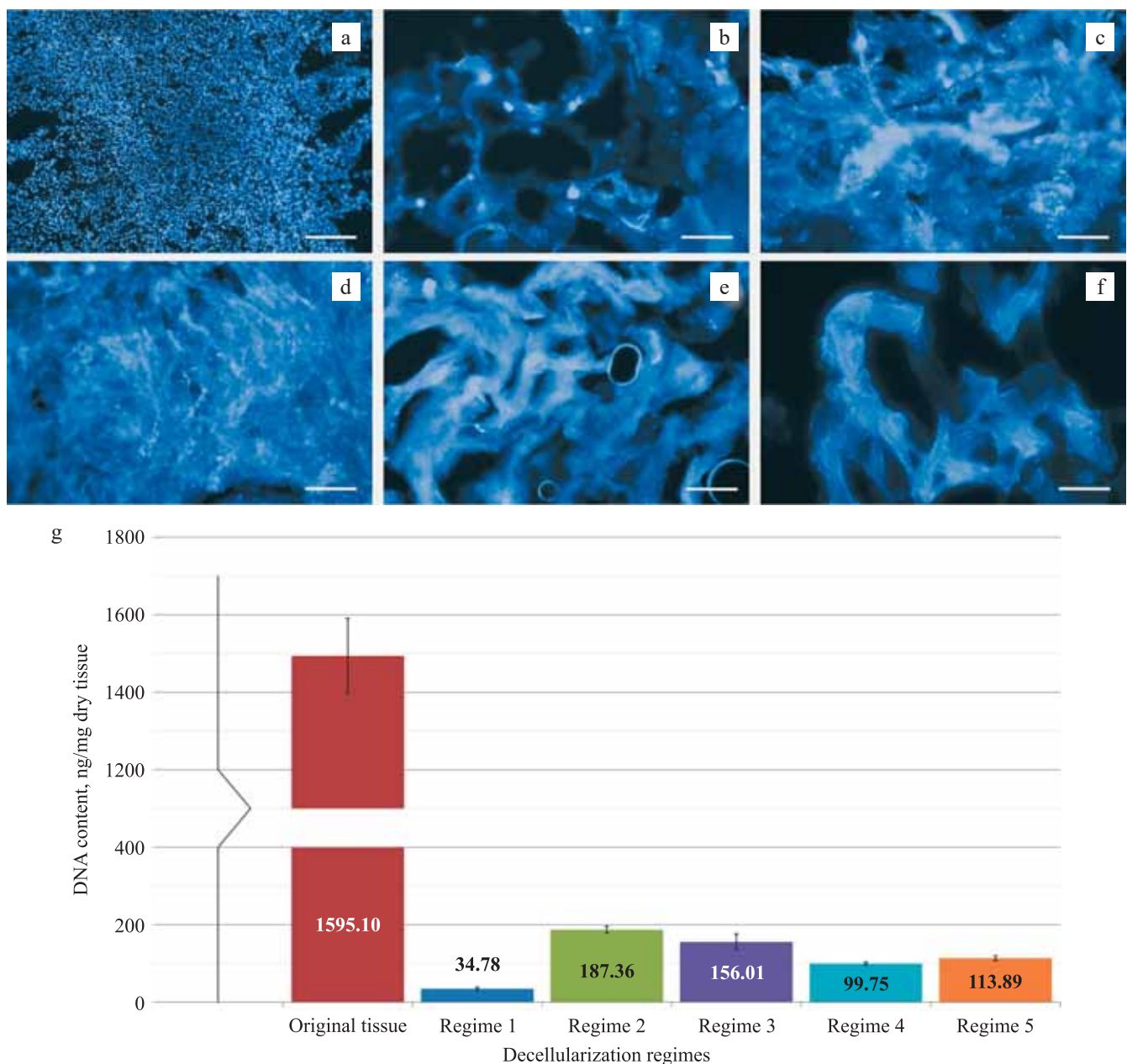


Fig. 2. Effect of porcine liver decellularization regime on DNA content. DAPI staining: a, original porcine liver tissue; b, regime 1; c, regime 2; d, regime 3; e, regime 4; f, regime 5. Scale bar, 100 µm. g, quantitative DNA content in porcine liver fragments

DPLF treated under regime 4 (Fig. 3, d–f) exhibited dense fiber arrangement with reduced porosity due to the formation of liver fragment conglomerates. The sample stained positively for total collagen (Masson’s method) and GAG (Alcian blue) (Fig. 3, e, f). However, preserved cellular detritus was observed.

Histological analysis aligned with DNA and GAG quantification data, demonstrating high GAG retention but insufficient DNA removal in DPLF obtained under regime 4.

To address this, additional treatment with type I DNAase solution was applied. Fig. 4 shows that this further reduced DNA levels to 0.94% of the original amount (14.93 ± 4.91 ng/mg dry tissue from 1595.10 ± 96.80 ng/mg dry tissue), significantly enhancing.

Based on these findings, decellularization regime 4 was selected as the optimal protocol due to its ability to maximize ECM structure preservation, retain high GAG content, and enhance cell and cellular debris removal.

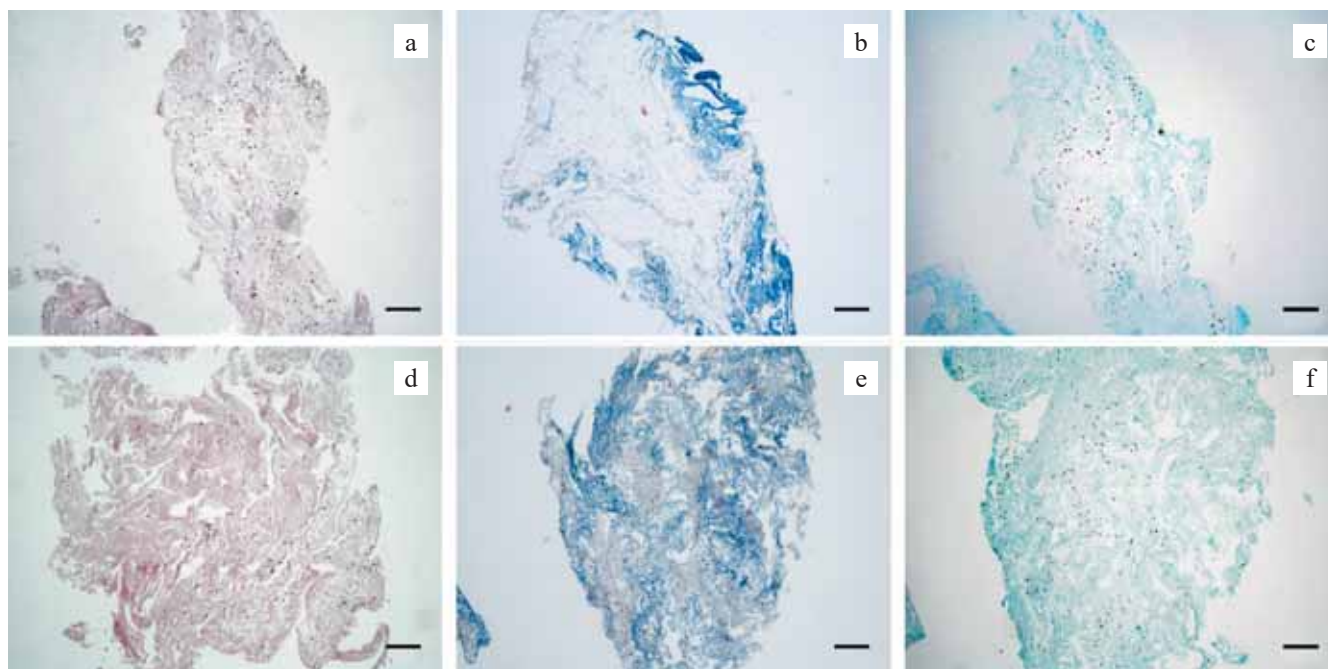


Fig. 3. Effect of porcine liver treatment regime on decellularization efficiency. H&E stain: a, regime 1; d, regime 4. Masson’s trichrome stain: b, regime 1; e, regime 4. Alcian blue stain: c, regime 1; f, regime 4. Scale bar, 100 µm

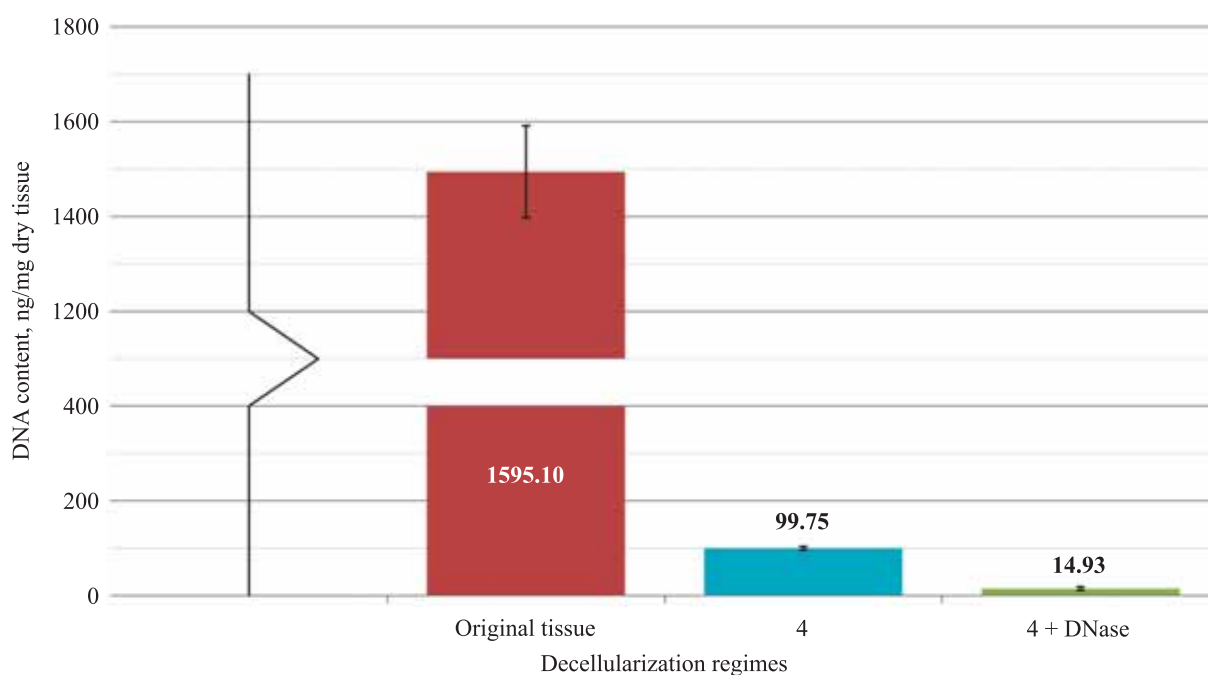


Fig. 4. Effect of DNase treatment on porcine liver decellularization efficiency

Cytotoxicity assessment of DPLF using the direct contact method on NIH/3T3 mouse fibroblast cultures demonstrated no adverse effects on cell morphology or

viability. As shown in Fig. 5, a, the number of viable fibroblasts was comparable to the negative control (Fig. 5, c). A cytotoxic effect was observed in the positive

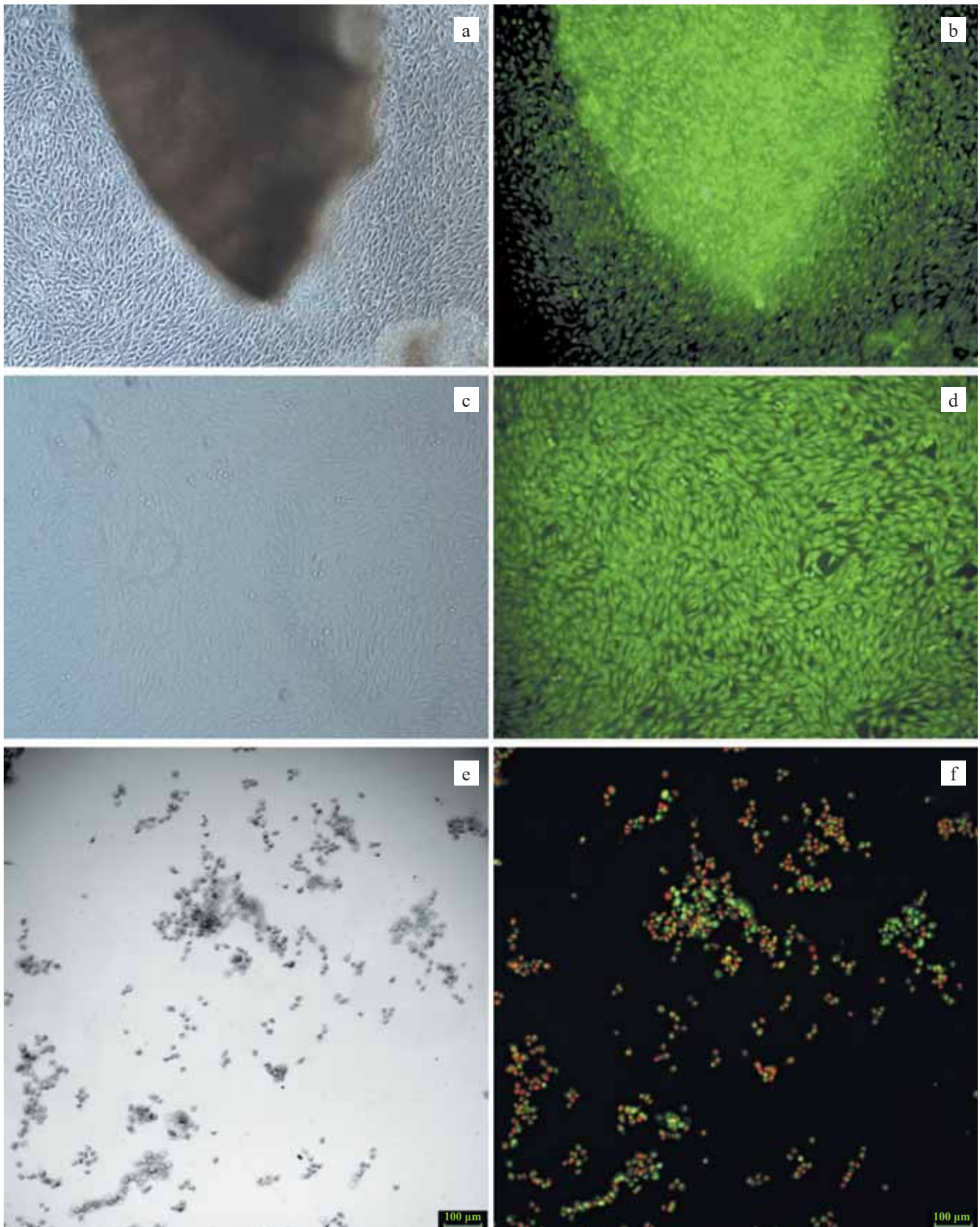


Fig. 5. Degree of cytotoxicity of matrix based on decellularized porcine liver fragments (DPLF) obtained in regime 4, *in vitro*. (a, b), test sample of DPLF; (c, d), negative control; (e, f), positive control. (a, c, e), phase-contrast microscopy; (b, d, f), fluorescence microscopy with LIVE/DEAD vital dye. 40× magnification

control sample, where cells exhibited a spherical shape, indicating loss of viability (Fig. 5, e).

The absence of cytotoxicity in DPLF obtained via decellularization regime 4 was further confirmed by LIVE/DEAD staining (Fig. 5, b). A large number of viable cells, forming a monolayer comparable to the negative control, were observed in contact with the samples (Fig. 5, d). The positive control (Fig. 5, e) exhibited dead cells with red fluorescence.

Based on these findings, it was concluded that DPLF has no cytotoxic effect *in vitro*.

CONCLUSION

Thus, our study revealed that SDS treatment negatively affected preservation of GAG, a key component of the natural ECM. However, optimization of the chemical porcine liver decellularization regime – through a two-stage application of surfactants and osmoregulators – successfully reduced tissue processing time by nearly half, enhanced ECM structure preservation, and reduced cellular component content, ensuring low potential immunogenicity and eliminating cytotoxic effects.

The authors declare no conflict of interest.

REFERENCES

- Dai Q, Jiang W, Huang F, Song F, Zhang J, Zhao H. Recent advances in liver engineering with decellularized scaffold. *Front Bioeng Biotechnol.* 2022; 10: 831477. doi: 10.3389/fbioe.2022.831477.
- Zhang X, Chen X, Hong H, Hu R, Liu J, Liu C. Decellularized extracellular matrix scaffolds: Recent trends and emerging strategies in tissue engineering. *Bioact Mater.* 2021; 10: 15–31. doi: 10.1016/j.bioactmat.2021.09.014.
- Isaeva EV, Beketov EE, Arguchinskaya NV, Ivanov SA, Shegay PV, Kaprin AD. Decellularized Extracellular Matrix for Tissue Engineering (Review). *Sovrem Tekhnologii Med.* 2022; 14 (3): 57–68. doi: 10.17691/stm2022.14.3.07.
- Garcia-Gareta E, Abduldaem Y, Sawadkar P, Kyriakidis C, Lali F, Greco KV. Decellularised scaffolds: just a framework? Current knowledge and future directions. *J Tissue Eng.* 2020; 11: 2041731420942903. doi: 10.1177/2041731420942903.
- Biomimetics of Extracellular Matrices for Cell and Tissue Engineered Medical Products / Ed. V.I. Sevastianov, Yu.B. Basok. Newcastle upon Tyne, UK: Cambridge Scholars Publishing, 2023; 339.
- Sodhi H, Panitch A. Glycosaminoglycans in tissue engineering: a review. *Biomolecules.* 2020; 11 (1): 29. doi: 10.3390/biom11010029.
- Huang Z, Godkin O, Schulze-Tanzil G. The challenge in using mesenchymal stromal cells for recellularization of decellularized cartilage. *Stem Cell Rev Rep.* 2017; 13 (1): 50–67. doi: 10.1007/s12015-016-9699-8.
- Neishabouri A, Soltani Khaboushan A, Daghigh F, Kajbafzadeh AM, Majidi Zolbin M. Decellularization in tissue engineering and regenerative medicine: evaluation, modification, and application methods. *Front Bioeng Biotechnol.* 2022; 10: 805299. doi: 10.3389/fbioe.2022.805299.
- Jeong W, Kim MK, Kang HW. Effect of detergent type on the performance of liver decellularized extracellular matrix-based bio-inks. *J Tissue Eng.* 2021; 12: 2041731421997091. doi: 10.1177/2041731421997091.
- Willemse J, Versteegen MMA, Vermeulen A, Schurink IJ, Roest HP, van der Laan LJW, de Jonge J. Fast, robust and effective decellularization of whole human livers using mild detergents and pressure controlled perfusion. *Mater Sci Eng C Mater Biol Appl.* 2020; 108: 110200. doi: 10.1016/j.msec.2019.110200.
- Nemets EA, Malkova AP, Duhina GA, Lazhko AJe, Basok YuB, Kirillova AD, Sevastianov VI. Effect of supercritical carbon dioxide on the *in vivo* biocompatible and resorptive properties of tissue-specific scaffolds from decellularized pig liver fragments. *Promising materials.* 2021; 11: 20–31. [In Russ, English abstract]. doi: 10.30791/1028-978X-2021-11-20-31.
- Gilpin A, Yang Y. Decellularization strategies for regenerative medicine: from processing techniques to applications. *Biomed Res Int.* 2017; 2017: 9831534. doi: 10.1155/2017/9831534.
- Syed O, Walters NJ, Day RM, Kim HW, Knowles JC. Evaluation of decellularization protocols for production of tubular small intestine submucosa scaffolds for use in oesophageal tissue engineering. *Acta Biomater.* 2014; 10 (12): 5043–5054. doi: 10.1016/j.actbio.2014.08.024.
- Sevastianov VI, Basok YuB, Grigoriev AM, Nemets EA, Kirillova AD, Kirsanova LA et al. Decellularization of cartilage microparticles: Effects of temperature, supercritical carbon dioxide and ultrasound on biochemical, mechanical, and biological properties. *J Biomed Mater Res A.* 2023; 111 (4): 543–555. doi: 10.1002/jbm.a.37474.
- Bakhtiar H, Rajabi S, Pezeshki-Modaress M, Ellini MR, Panahinia M, Alijani S et al. Optimizing methods for bovine dental pulp decellularization. *J Endod.* 2021; 47 (1): 62–68. doi: 10.1016/j.joen.2020.08.027.
- Kobes JE, Georgiev GI, Louis AV, Calderon IA, Yoshimaru ES, Klemm LM et al. A comparison of iron oxide particles and silica particles for tracking organ recellularization. *Mol Imaging.* 2018; 17: 1536012118787322. doi: 10.1177/1536012118787322.
- Kim JK, Koh YD, Kim JO, Seo DH. Development of a decellularization method to produce nerve allografts using less invasive detergents and hyper/hypotonic solutions. *J Plast Reconstr Aesthet Surg.* 2016; 69 (12): 1690–1696. doi: 10.1016/j.bjps.2016.08.016.
- Crapo PM, Gilbert TW, Badylak SF. An overview of tissue and whole organ decellularization processes. *Biomaterials.* 2011; 32 (12): 3233–3243. doi: 10.1016/j.biomaterials.2011.01.057.
- Suss PH, Ribeiro VST, Motooka CE, de Melo LC, Tuon FF. Comparative study of decellularization techniques to obtain natural extracellular matrix scaffolds of human peripheral-nerve allografts. *Cell Tissue Bank.* 2022; 23 (3): 511–520. doi: 10.1007/s10561-021-09977-x.
- Nemets EA, Kirsanova LA, Basok JB, Schagidulin MJ, Volkova EA, Metelsky ST, Sevastianov VI. Technology

- features of decellularization of human liver fragments as tissue-specific fine-grained matrix for cell-engineering liver construction. *Russian Journal of Transplantology and Artificial Organs*. 2017; 19 (4): 70–77. [In Russ, English abstract]. doi: 10.15825/1995-1191-2017-4-70-77.
21. Kirillova AD, Basok YB, Lazhko AE, Grigoryev AM, Kirsanova LA, Nemets EA, Sevastianov VI. Creating a tissue-specific microdispersed matrix from a decellularized porcine liver. *Physics and Chemistry of Materials Processing*. 2020; 4: 41–50. [In Russ, English abstract]. doi: 10.30791/0015-3214-2020-4-41-50.
 22. GOST ISO 10993-5-2011. Medical devices. Biological evaluation of medical devices. Part 5. Tests for *in vitro* cytotoxicity. M.: Standartinform, 2014; 9.
 23. Gordillo M, Evans T, Gouon-Evans V. Orchestrating liver development. *Development*. 2015; 142 (12): 2094–2108. doi: 10.1242/dev.114215.
 24. Zhou J, Fritze O, Schleicher M, Wendel HP, Schenke-Layland K, Harasztosi C et al. Impact of heart valve decellularization on 3-D ultrastructure, immunogenicity and thrombogenicity. *Biomaterials*. 2010; 31 (9): 2549–2554. doi: 10.1016/j.biomaterials.2009.11.088.
 25. O'Neill JD, Anfang R, Anandappa A, Costa J, Javidfar J, Wobma HM et al. Decellularization of human and porcine lung tissues for pulmonary tissue engineering. *Ann Thorac Surg*. 2013; 96 (3): 1046–1056. doi: 10.1016/j.athoracsur.2013.04.022.
 26. Sullivan DC, Mirmalek-Sani SH, Deegan DB, Baptista PM, Aboushwareb T, Atala A, Yoo JJ. Decellularization methods of porcine kidneys for whole organ engineering using a high-throughput system. *Biomaterials*. 2012; 33 (31): 7756–7764. doi: 10.1016/j.biomaterials.2012.07.023.

The article was submitted to the journal on 17.08.2024